Volume 58(8): 707–719, 2010
Journal of Histochemistry & Cytochemistry
http://www.jhc.org

ARTICLE

Spatial, Cellular, and Intracellular Localization of Na^+/K^+-ATPase in the Sterically Disposed Renal Tubules of Japanese Eel

Keitaro Teranishi and Toyoji Kaneko

Department of Aquatic Bioscience, Graduate School of Agricultural and Life Sciences, The University of Tokyo, Bunkyo, Tokyo, Japan

SUMMARY The kidney plays a crucial role in the regulation of water and ion balances in both freshwater and seawater fishes. However, the complicated structures of the kidney hamper comprehensive understanding of renal functions. In this study, to investigate the structure of sterically disposed renal tubules, we examined spatial, cellular, and intracellular localization of Na^+/K^+-ATPase in the kidney of the Japanese eel. The renal tubule was composed of the first (PT-I) and second (PT-II) segments of the proximal tubule and the distal tubule (DT), followed by the collecting ducts (CDs). Light microscopic immunocytochemistry detected Na^+/K^+-ATPase along the renal tubules and CD; however, the subcellular distribution of the Na^+/K^+-ATPase immunoreaction varied among different segments. Electron microscopic immunocytochemistry further revealed that Na^+/K^+-ATPase was distributed on the basal infoldings of PT-I, PT-II, and DT cells. Three-dimensional analyses showed that the renal tubules meandered in a random pattern through lymphoid tissues, and then merged into the CD, which was aligned linearly. Among the different segments, the DT and CD cells showed more-intense Na^+/K^+-ATPase immunoreaction in freshwater eel than in seawater-acclimated eel, confirming that the DT and CD segments are important in freshwater adaptation, or hyperosmoregulation. **(J Histochem Cytochem 58:707–719, 2010)**

KEY WORDS
kidney
Na^+/K^+-ATPase
renal tubule
spatial alignment
eel
osmoregulation

TELEOST FISHES MAINTAIN the osmolality of their body fluid within narrow physiological ranges, equivalent to about one-third seawater osmolality, independent of environmental salinities. In teleosts, the gill, kidney, and intestine are important osmoregulatory organs, creating osmotic and ionic gradients between the body fluid and external environments (Marshall and Grosell 2006). Among them, the kidney plays a crucial role in regulation of water and ion balances in both freshwater and seawater fish, although its function is entirely different between hypo- and hypertonic conditions. The kidney (body kidney) of teleosts is generally composed of numerous nephrons and the infilling lymphoid tissues. The nephron, acting as a functional unit for renal osmoregulation, consists of a renal corpuscle (a Bowman's capsule and a glomerulus), proximal tubule (PT), and distal tubule (DT), followed by a collecting duct (CD). Freshwater teleosts face osmotic water load and ion loss through their permeable body surfaces. To deal with the osmotic problems, the kidney in freshwater fish produces a large amount of dilute urine by filtering a large quantity of blood in glomeruli and reabsorbing ions from the filtrate in renal tubules. Conversely, seawater teleosts face osmotic water loss and ion load. To overcome the water and ion disturbances, the kidney in seawater fish excretes excess divalent ions but produces a relatively small amount of isotonic urine to minimize water loss (Hickman 1968).

Recently, the molecular mechanisms of osmoregulatory functions of gill mitochondria-rich cells, also referred to as chloride cells, have become increasingly clear. Molecular studies have revealed various

Correspondence to: Keitaro Teranishi, Department of Aquatic Bioscience, Graduate School of Agricultural and Life Sciences, The University of Tokyo, 1-1-1 Yayoi, Bunkyo, Tokyo 113-8657, Japan. E-mail: teranishi@marine.fs.a.u-tokyo.ac.jp

Received for publication November 18, 2009; accepted April 9, 2010 [DOI: 10.1369/jhc.2010.955492].

ion transport proteins expressed in the gill mitochondria-rich cells, and their expression profiles in fish acclimated to freshwater and seawater (Hirose et al. 2003; Hwang and Lee 2007; Hiroi et al. 2008; Inokuchi et al. 2008). However, although molecular information on renal ion and water transports has been accumulated (Miyazaki et al. 2002; Katoh et al. 2006; Cutler and Cramb 2008), the complicated structures of the kidney hamper comprehensive understanding of renal functions. The morphology of the fish kidney has been described repeatedly in old literature (e.g., Anderson and Loewen 1975); however, few studies have successfully depicted the spatial structure of the nephrons and their positional relationship. For a better understanding of fish renal functions, it is profitable to reinvestigate the morphology of nephrons, in particular, the structure of sterically disposed renal tubules, by using more sophisticated techniques. Such an attempt enables us to correlate molecular information on ion transport proteins involved in renal osmoregulation with morphological information on cellular and subcellular distribution of those ion transporters in different segments of the renal tubules that run spatially in the kidney.

The major functional significance of renal tubules in osmoregulation lies in reabsorption and secretion of monovalent and divalent ions to maintain ion balances of the body fluid in fish inhabiting various ionic and osmotic environments. It is well accepted that electrochemical gradients created by Na^+/K^+-ATPase are widely used for various ion transport systems (Geering 1990). As is the case with gill mitochondria-rich cells, active ion transports in renal tubules are also driven by electrochemical gradients created by electrogenic ion transporters such as Na^+/K^+-ATPase (Nishimura and Fan 2003). Thus, the protein expression and localization of Na^+/K^+-ATPase could be a useful indicator of ion transport activities in renal tubules.

In the present study, we aimed to investigate the spatial, cellular, and intracellular localization of Na^+/K^+-ATPase in the sterically disposed renal tubules in the kidney of the Japanese eel, *Anguilla japonica*, using various techniques, such as conventional light and electron microscopy, light and electron microscopic immunocytochemistry for Na^+/K^+-ATPase, and confocal laser scanning microscopy. We also compared the distribution of Na^+/K^+-ATPase in renal tubules between freshwater- and seawater-acclimated eels to clarify morphological alteration and functional diversity of the renal tubule in hypo- and hypertonic environments.

Materials and Methods

Fish and Sampling

Cultured Japanese eels, weighing ~200 g, were obtained from a commercial supplier (Taketune; Hamamatsu, Japan). Eels were maintained in tanks supplied with recirculating freshwater. To prepare seawater-acclimated eels, freshwater-acclimated eels were transferred to full-strength seawater after pre-acclimation to 50%-diluted seawater for 2 days. The fish were maintained in seawater for at least 2 weeks. The temperature was maintained at 20C and the fish were not fed during this period. After anesthesia with 0.2% 2-phenoxyethanol, the kidney was dissected out from freshwater- and seawater-acclimated eels for the following experiments. Three fish were allotted for each experiment, and the fish used for various histological techniques were different ones. Experiments were conducted according to the principles and procedures approved by the Institutional Animal Care and Use Committee of the University of Tokyo.

Antiserum and Western Blot Analysis

For the detection of renal tubules and CDs in the kidney, we used an antiserum specific for Na^+/K^+-ATPase. The antiserum (NAK121) was raised in a rabbit against a synthetic peptide corresponding to part of the highly conserved region of the Na^+/K^+-ATPase α-subunit (Uchida et al. 2000). The specificity of the antiserum was confirmed by Western blot analysis according to the methods of Katoh et al. (2000) and Watanabe et al. (2008), with some minor modifications. The kidney from freshwater-acclimated eel was homogenized with a PT-1200E homogenizer (Polytron; Lucerne, Switzerland) on ice in homogenization buffer [25 mM Tris-HCl (pH 7.4), 0.25 M sucrose, 1 tablet of Complete-Mini, EDTA-free (Roche Diagnostics; Basel, Switzerland) per 10 ml]. The homogenate was centrifuged at 9000 × g for 30 min at 4C, and the supernatant was collected as protein samples for Western blot analysis. The samples were solubilized in 2× sample loading buffer [100 mM Tris-HCl (pH 6.8), 4% SDS, 20% glycerol, 0.02% bromophenol blue, 10% 2-mercaptoethanol] and heated at 70C for 15 min. The resulting protein samples were separated by SDS-polyacrylamide gel electrophoresis. After electrophoresis, the protein was transferred from the gel to a polyvinylidine difluoride membrane (Immobilon-P Transfer Membrane; Millipore, Billerica, MA). After blocking with blocking buffer [5% skim milk in 50 mM TBS containing 0.1% Tween-20 (TBST)] for 30 min at room temperature, the membrane was incubated with anti-Na^+/K^+-ATPase diluted 1:1000 with blocking buffer overnight at 4C. The membrane was rinsed with TBST, and then incubated with horseradish peroxidase (HRP)-linked anti-rabbit IgG (Cell Signaling Technology; Beverly, MA) diluted 1:10,000 with blocking buffer for 3 hr at room temperature. The immunoreactive band was detected using Immobilon Western chemiluminescent HRP substrate (Millipore) according to the manufacturer's instructions.

Light Microscopic Immunocytochemistry

To examine the morphology of different renal tubule segments, paraffin sections of the kidney were stained immunocytochemically with anti-Na^+/K^+-ATPase. The kidneys from freshwater- and seawater-acclimated eels (n=3 each) were fixed in 4% paraformaldehyde (PFA) in 0.1 M phosphate buffer (PB; pH 7.4) overnight at 4C, and stored in 70% ethanol. The fixed kidney was dehydrated in ethanol and embedded in Paraplast (McCormick Scientific; Richmond, IL). Serial cross-sections cut at 4-μm thickness were divided into two groups and mounted on separate MAS-coated slides (Matsunami Glass; Osaka, Japan). One set of sections was immunostained with anti-Na^+/K^+-ATPase by the avidin-biotin-peroxidase complex (ABC) method (Hsu et al. 1981) using the Vectastain ABC kit (Vector Laboratories; Burlingame, CA) as described in Uchida et al. (1996). In brief, deparaffined sections were incubated sequentially with: (1) 0.6% H_2O_2 for 30 min; (2) 2% normal goat serum (NGS) in 0.01 M PBS (pH 7.4) for 30 min; (3) anti-Na^+/K^+-ATPase diluted 1:2000 with PBS containing 2% normal goat serum (NGS), 0.1% BSA, 0.02% keyhole limpet hemocyanin (KLH), and 0.01% sodium azide overnight at 4C; (4) biotinylated anti-rabbit IgG for 30 min; (5) ABC for 1 hr; and (6) 0.02% DAB containing 0.005% H_2O_2 for 5 min. Another set of sections was subjected to periodic acid-Schiff (PAS) stain and counterstain with hematoxylin. The specificity of the immunoreaction was confirmed by a control experiment in which the sections were incubated with the preimmune serum in place of the antiserum.

Transmission Electron Microscopy

The kidney was dissected out from freshwater- and seawater-acclimated eels (n=3 each), cut into small pieces, and fixed in 2% PFA–2% glutaraldehyde (GA) in 0.1 M PB for 3 hr at room temperature. After rinsing in 0.1 M PB, the tissues were postfixed in 1% osmium tetroxide in 0.1 M PB for 1 hr at room temperature. The tissues were dehydrated in ethanol, transferred to propylene oxide, and embedded in Spurr's resin (Polysciences; Warrington, PA). Ultrathin sections were cut with a diamond knife and mounted on grids. The sections were stained with uranyl acetate and lead citrate, and examined with a transmission electron microscope (JEM1010; JEOL, Tokyo, Japan).

Electron Microscopic Immunocytochemistry

The kidney was dissected out from freshwater-acclimated eel (n=3), and fixed in 2% PFA–0.2% GA in 0.1 M PB for 6 hr at room temperature. The fixed kidney was sliced at 200-μm thickness with a microslicer (DTK-2000; Dosaka EM, Kyoto, Japan). The sliced kidney was immunocytochemically stained by the ABC method with the Vectastain ABC kit (Vector Laboratories). In brief, the sliced tissues were incubated sequentially with: (1) 0.6% H_2O_2 for 30 min; (2) 2% NGS for 30 min; (3) anti-Na^+/K^+-ATPase diluted 1:500 with PBS containing 10% NGS, 0.1% BSA, 0.02% KLH, 0.05% Triton X-100, and 0.01% sodium azide (NB-PBS) for 2 days at 4C; (4) biotinylated anti-rabbit IgG for 20 hr at 4C; (5) ABC for 20 hr at 4C; and (6) 0.02% DAB containing 0.005% H_2O_2 for 30 min. The tissues were then postfixed in 1% osmium tetroxide in 0.1 M PB for 15 min. After dehydration in ethanol, the sections were embedded in Spurr's resin. Ultrathin sections were cut with a diamond knife and mounted on grids. The specimens were observed with the JEM1010 transmission electron microscope. The specificity of the immunoreaction was confirmed by a control experiment in which the sections were incubated with the preimmune serum in place of the antiserum.

Reconstruction of the Spatial Structure of Nephrons From Serial Sections

To elucidate the whole structure of the nephron, we traced single nephrons through serial sections of the kidney covering ~600-μm thickness. The kidney from freshwater-acclimated eel was fixed in 4% PFA and embedded in Paraplast as described above (n=3). Serial sagittal sections were cut at 8-μm thickness and mounted on MAS-coated slides. The sections were immunocytochemically stained with anti-Na^+/K^+-ATPase as described above, and counterstained with hematoxylin. The serial sections were observed under a light microscope (E800; Nikon, Tokyo, Japan) equipped with a differential interference device. Serial images were photographed and used for the reconstruction of the nephron structure. Single nephrons appearing over serial sections were traced with the aid of Photoshop software (Adobe Systems; Tokyo, Japan) to obtain the overlaid images.

Confocal Laser Scanning Microscopy

Whole-mount samples of the sliced kidney were immunocytochemically stained with anti-Na^+/K^+-ATPase and examined by confocal laser scanning microscopy. The kidney from freshwater-acclimated eel was fixed in 4% PFA as described above (n=3). The fixed kidney was sliced at 200-μm thickness with the microslicer. The sliced kidney was then incubated with anti-Na^+/K^+-ATPase diluted 1:500 with NB-PBS for 3 days at 4C. After rinsing in PBS, the samples were then incubated with Alexa Fluor 555–labeled goat anti-rabbit IgG (Invitrogen; Eugene, OR) diluted 1:1000 with PBS for 3 days at 4C. For the detection of brush borders, some samples were further incubated with Alexa Fluor 488–labeled wheat germ agglutinin (WGA; Invitrogen) at a concentration of 2 μg/ml in PBS overnight at 4C. It

is known that WGA selectively binds to glycoconjugates (Wright 1984). Because brush borders are coated with a glycocalyx, WGA serves as a marker for brush borders in renal tubules. In addition, it has been shown that WGA specifically detects the glomeruli in the kidney (Ojeda et al. 2003). After rinsing in PBS, the samples were mounted on glass slides and examined with a confocal laser scanning microscope (C1; Nikon). The wavelengths of excitation and recorded emission for Alexa dyes were as follows: Alexa Fluor 488, 488 nm and 515/30 nm; and Alexa Fluor 555, 543 nm and 605/75 nm. We performed z-stacks with optical sections over 200-μm thickness.

Dissociation of Nephrons

To observe the nephron structure from another point of view, single nephrons were dissociated from the kidney according to the method of Evan et al. (1976) with some modifications. The kidney from freshwater-acclimated eels (n=3) was fixed in 4% PFA as described above, and cut into small pieces. After rinsing in 0.1 M PB, the tissues were treated with 8 N HCl for 40 min at 60C, followed by rinsing three times (5 min each) in 0.1 M PB. Single nephrons were raveled out with fine forceps under a dissecting microscope, and observed under a Nikon E800 microscope.

Results

Western Blot Analysis

In Western blot analysis, the antiserum raised in a rabbit against the synthetic peptide corresponding to part of the highly conserved region of the Na^+/K^+-ATPase α-subunit recognized a major protein band with a molecular mass of ~100 kDa (Figure 1).

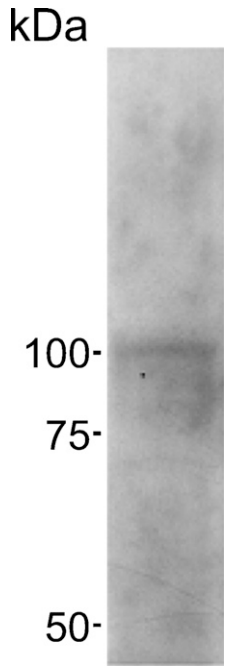

Figure 1 Western blot analysis for Na^+/K^+-ATPase expressed in the kidney of freshwater-acclimated eel. Positions for molecular mass markers are shown on the left.

General Structure of Renal Tubules

The general structure of the renal tubules was first observed on paraffin sections. In the kidneys of both freshwater- and seawater-acclimated eels, the renal tubule was mainly composed of three regions: the first (PT-I) and second (PT-II) segments of the PT, and the DT. The PT segments consisted of a single layer of columnar epithelial cells, with a nucleus located basolaterally in PT-I cells and centrally in PT-II cells (Figures 2A, 2B, 2I, and 2J). The apical membranes of those cells composing PT segments were equipped with a PAS-positive brush border. The brush border was thicker in the PT-I segment than in the PT-II segment. On the other hand, the DT segment was composed of a single layer of cuboidal epithelial cells with a centrally located nucleus and lacked a brush border at the apical side (Figures 2C and 2K). The following CD segment consisted of a single layer of columnar epithelial cells with a centrally located nucleus, and was distinguished from the other segments by the presence of surrounding connective tissues (Figures 2D and 2L). Similar to the DT segment, the CD cells lacked a PAS-positive brush border at the apical membrane.

Distribution of Na^+/K^+-ATPase Along the Renal Tubule and CD in Freshwater- and Seawater-acclimated Eels

The immunoreaction for Na^+/K^+-ATPase was detected all along the renal tubules and CDs; however, the subcellular distribution of the Na^+/K^+-ATPase immunoreaction varied among different segments and between freshwater- and seawater-acclimated eels (Figures 2E–2H, 2M–2P, 2Q, and 2R). In freshwater-acclimated fish, whereas faint Na^+/K^+-ATPase immunoreaction was restricted to the subcellular region along the basolateral membrane in the PT-I and PT-II cells (Figures 2E and 2F), intense immunoreaction was observed over the cytoplasm, with the nucleus and subapical region unstained in the DT cells (Figure 2G). In the CD cells of freshwater fish, the distribution pattern of the Na^+/K^+-ATPase immunoreaction was similar to that of the DT cells, but the intensity of the immunoreaction was apparently less than that in the DT cells (Figure 2H). Whereas no distinct difference was seen in PT-I and PT-II cells between freshwater and seawater fish (Figures 2E, 2F, 2M, and 2N), the Na^+/K^+-ATPase immunoreaction in DT and CD cells was weaker in seawater fish than in freshwater fish (Figures 2G, 2H, 2O, and 2P). The distribution of the immunoreaction

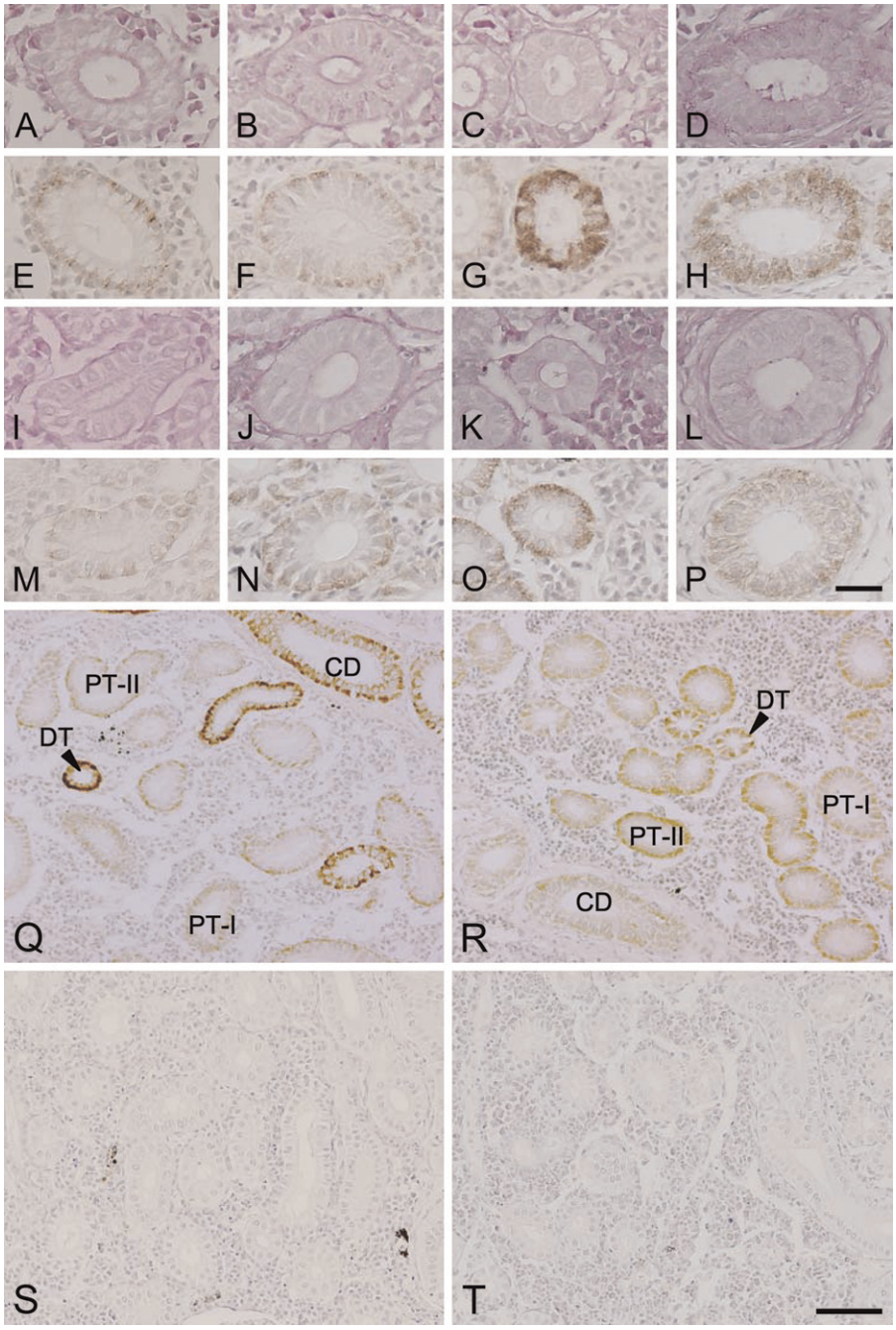

Figure 2 Light micrographs of the first (**A,E,I,M**) and second (**B,F,J,N**) segments of the proximal tubules, distal tubules (**C,G,K,O**), and collecting ducts (**D,H,L,P**) in the kidneys of freshwater (**A–H**)- and seawater (**I–P**)-acclimated eels. Adjacent sections were stained with periodic acid-Schiff stain (**A–D,I–L**) and anti-Na^+/K^+-ATPase (**E–H,M–P**). Low-magnification views of the kidney sections (**Q–T**) stained with anti-Na^+/K^+-ATPase (**Q,R**) or with the preimmune serum as controls (**S,T**) in freshwater (**Q,S**)- and seawater (**R,T**)-acclimated eels. PT-I, first segment of proximal tubule; PT-II, second segment of proximal tubule; DT, distal tubule; CD, collecting duct. Bars: **A–P** = 20 μm; **Q–T** = 50 μm.

was restricted to the basal half of the cells in seawater fish, whereas it extended to the apical half of the DT and CD cells in freshwater fish. The control experiment, in which the sections were incubated with the preimmune serum in place of the antiserum, resulted in complete extinction of the immunoreaction.

Electron Microscopic Observations on Renal Tubules

The fine structure of the cells in different segments of renal tubules was observed in freshwater- and seawater-acclimated eels by means of transmission electron microscopy. In accordance with the light microscopic observations, PT-I and PT-II segments were formed by columnar cells, with a basolaterally located nucleus in PT-I cells and a centrally located one in PT-II cells (Figures 3A, 3B, 4A, and 4B). The apical membranes of PT-I and PT-II cells possessed long and dense microvilli (Figures 3A, 3B, 4A, and 4B), which were observed as brush borders in the light microscopy. The microvilli in PT-I cells were

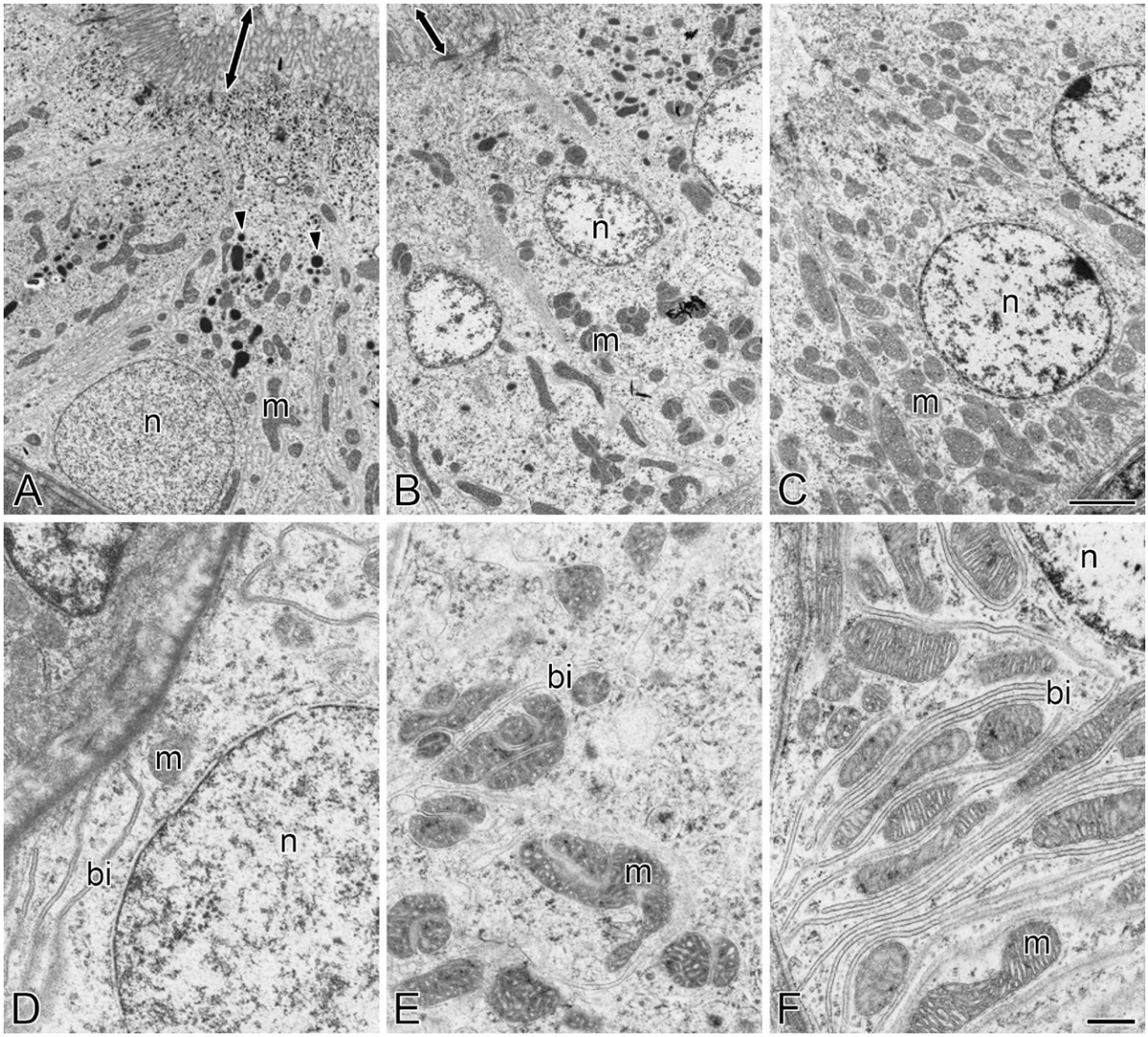

Figure 3 Transmission electron micrographs of the first (**A,D**) and second (**B,E**) segments of the proximal tubule and the distal tubule (**C,F**) in the kidney of freshwater-acclimated eel. Arrowheads and arrows indicate lysosomal granules and microvilli, respectively. bi, basal infolding; m, mitochondrion; n, nucleus. Bars: **A–C** = 2 μm; **D–F** = 500 nm.

longer and more dense than those in PT-II cells. The PT-I cells were also characterized by the presence of electron-dense lysosomal granules in the cytoplasm, whereas lysosomal granules were not observed in PT-II and DT cells (Figures 3A–3C and 4A–4C). Mitochondria were moderately developed in the cytoplasm of both PT-I and PT-II cells. The basal infolding continuous with the basolateral membrane was typically observed in the basal half of PT-I and PT-II cells. In contrast, DT cells were formed by cuboidal cells with a centrally located nucleus and scanty microvilli at the apical membrane (Figures 3C and 4C). The DT cells had a rich population of mitochondria, as compared with PT-I and PT-II cells. The basal infolding in DT cells was well developed and invaginated much more deeply than that in PT-I and PT-II cells (Figures 3D–3F and 4D–4F). No distinct difference was observed in the fine structures of renal tubule cells between freshwater and seawater eels.

Intracellular Localization of Na^+/K^+-ATPase in Different Segments of Renal Tubules

Electron microscopic immunocytochemistry revealed that Na^+/K^+-ATPase was distributed on the basal infoldings of PT-I, PT-II, and DT cells (Figures 5A–5C). The immunoreaction was detected neither in the apical

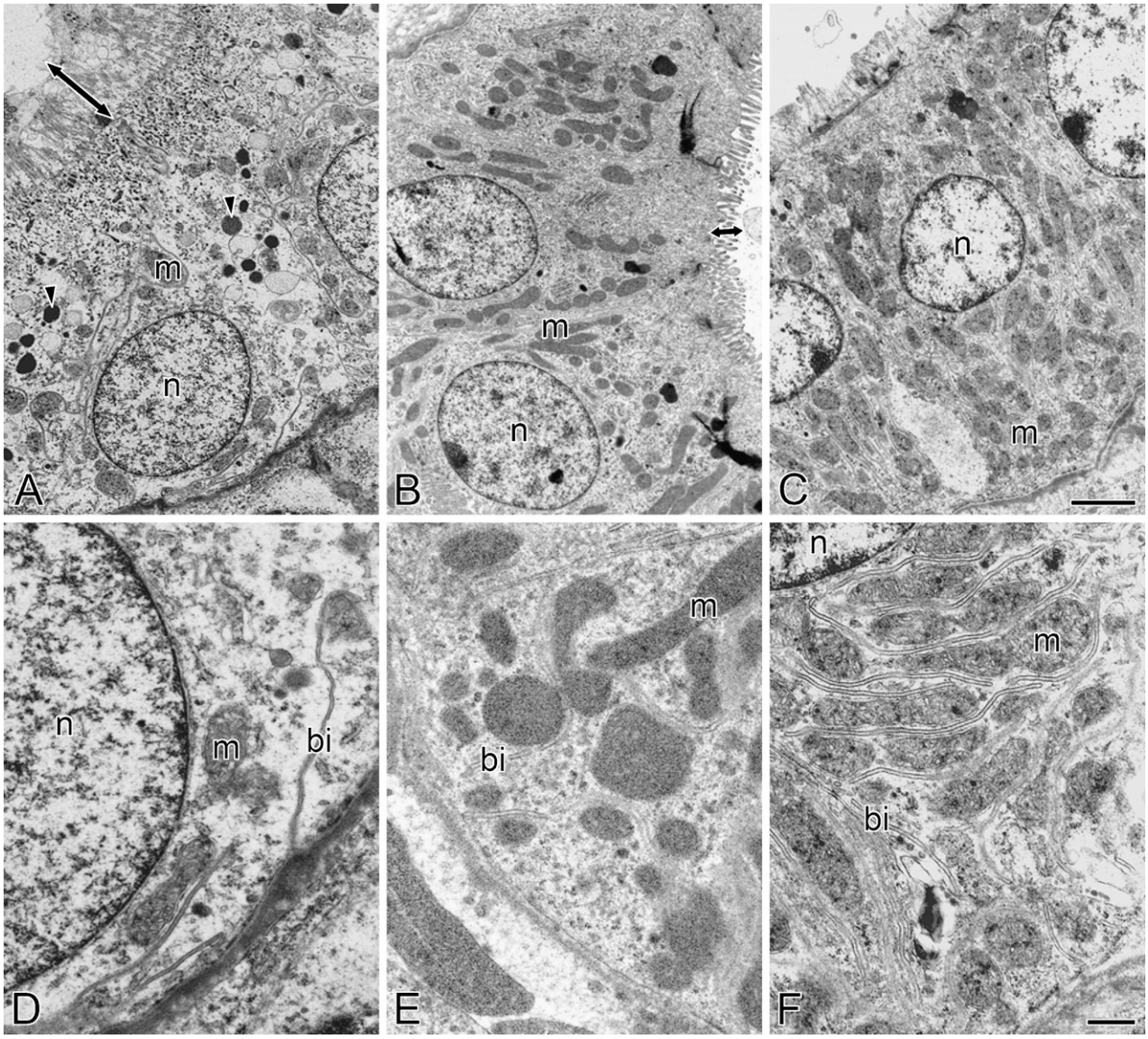

Figure 4 Transmission electron micrographs of the first (**A,D**) and second (**B,E**) segments of the proximal tubule and the distal tubule (**C,F**) in the kidney of seawater-acclimated eel. Arrowheads and arrows indicate lysosomal granules and microvilli, respectively. bi, basal infolding; m, mitochondrion; n, nucleus. Bars: **A–C** = 2 μm; **D–F** = 500 nm.

membrane nor in mitochondria and other organelles. Along with the densest distribution of the basal infolding in DT cells, Na^+/K^+-ATPase immunoreaction was most evident in DT cells, followed by PT-I and PT-II cells. No immunoreaction was seen in control specimens incubated with the preimmune serum (Figure 5D).

Spatial Alignment of Nephrons

The spatial alignment of the nephrons in freshwater-acclimated eel was examined by observations on serial sections immunostained with anti-Na^+/K^+-ATPase. Figure 6 depicts a series of representative sections (Figures 6A–6T) and the overlaid image (Figure 6U) of a single nephron. The renal tubule meandered in a random pattern through lymphoid tissues, and the distribution did not follow a regular pattern.

To further confirm the spatial distribution of the nephrons observed above, the kidney slices cut at 200-μm thickness were subjected to immunocytochemistry for Na^+/K^+-ATPase, and observed with a confocal laser scanning microscope. Although the slice did not cover a whole single nephron, the Na^+/K^+-ATPase-immunoreactive renal tubules were shown to run randomly in the kidney (Figure 7A). In the kidney slices that were double-stained with anti-Na^+/K^+-ATPase and WGA, renal tubules were labeled in red with

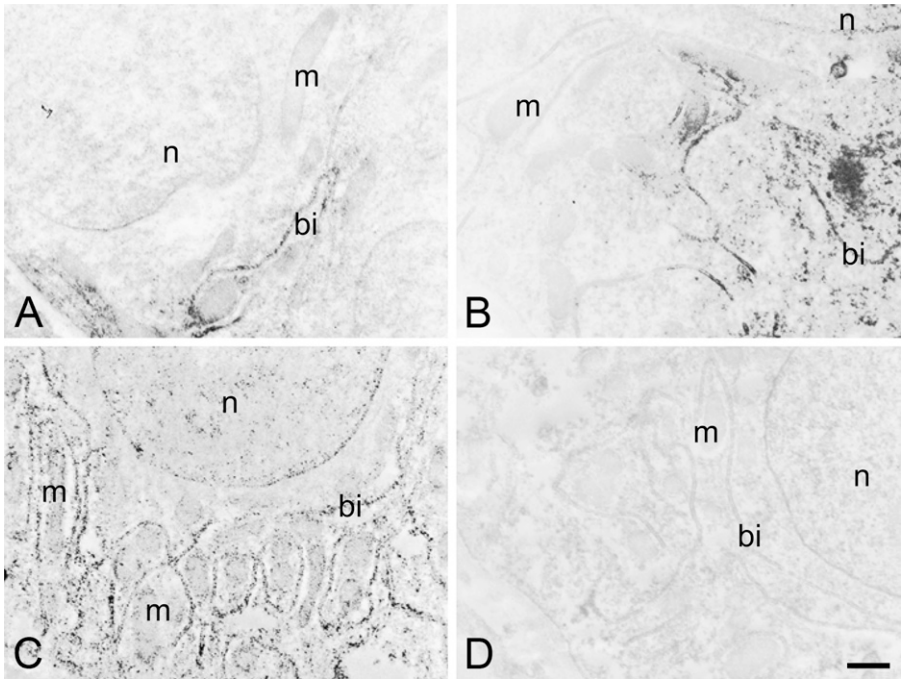

Figure 5 Electron microscopic immunocytochemistry of the kidney in freshwater-acclimated eel, incubated with anti-Na^+/K^+-ATPase (**A–C**) and the preimmune serum as a control (**D**). The immunoreaction was seen on the basal infoldings of the cells composing the first (**A**) and second (**B**) segments of the proximal tubule and the distal tubule (**C**), but absent in the control (a distal tubule cell) incubated with preimmune serum (**D**). bi, basal infolding; m, mitochondrion; n, nuclei. Bar = 500 nm.

anti-Na^+/K^+-ATPase, and the brush borders in the PT-I and PT-II segments and glomeruli in the renal corpuscle were labeled in green with WGA (Figure 7B). The PT-I and PT-II segments with relatively weak Na^+/K^+-ATPase immunoreaction restricted to the outer region of the tubules (the basal region of the cells) possessed WGA-positive brush borders in the apical side. Meanwhile, those cells in the DT and CD segments were intensely stained with anti-Na^+/K^+-ATPase and lacked WGA-positive brush borders.

Observations on Dissociated Single Nephrons

Because the dissociation procedures usually resulted in fragmentation of nephrons, few intact nephrons were obtained. Nevertheless, observations on fragments of dissociated nephrons also revealed a meandering feature of the renal tubules (Figure 8A). After meandering, the renal tubules were merged into the CD, which was aligned linearly (Figure 8B).

Discussion

For the immunocytochemical detection of Na^+/K^+-ATPase in the renal tubules and CD, we used the antiserum raised against a synthetic peptide corresponding to a highly conserved sequence of the Na^+/K^+-ATPase α-subunit (Uchida et al. 2000). This antiserum has been widely used for the detection of Na^+/K^+-ATPase in gill mitochondria-rich cells in various teleost species (Uchida et al. 2000; Lee et al. 2005; Hiroi and McCormick 2007; Sasai et al. 2007). In the present study, the specificity and availability of the antiserum were evaluated by Western blot analysis, in which the antiserum reacted with a major protein band of ~100 kDa, corresponding to the predicted molecular mass of Na^+/K^+-ATPase α-subunit (Hwang et al. 1998; Lucu and Flik 1999). This result indicates the high specificity of the antiserum for kidney Na^+/K^+-ATPase and its availability for immunocytochemical detection for Na^+/K^+-ATPase in the kidney of the Japanese eel.

In paraffin sections stained with PAS/hematoxylin, the PT-I, PT-II, DT, and CD segments in both freshwater- and seawater-acclimated eels were readily distinguished from each other by the following morphological characteristics: (1) the shape of the cells; (2) the location of the nuclei; and (3) the appearance of PAS-positive brush borders. Such morphological characteristics of different segments of the renal tubule and CD in the eel kidney are substantially in accordance with those observed in other teleost species, such as brook trout (*Salvelinus fontinalis*), rainbow trout (*Oncorhynchus mykiss*), and killifish (*Fundulus heteroclitus*) (Anderson and Loewen 1975; Katoh et al. 2008).

In our observations, the nephron of the Japanese eel possessed the distinct DT segment, which is responsible for reabsorption of monovalent ions in fish adapted to hypotonic environments (Marshall and Grosell 2006). In contrast, the euryhaline killifish lacks a DT segment or possesses only a short DT segment (Edwards and Schnitter 1933; Katoh et al. 2008), although this species is adaptable to freshwater environments (Katoh et al. 2001). It has been reported that mitochondria-rich cells in the gills and opercular membrane are larger in killifish adapted to freshwater than in those adapted

The Journal of Histochemistry & Cytochemistry

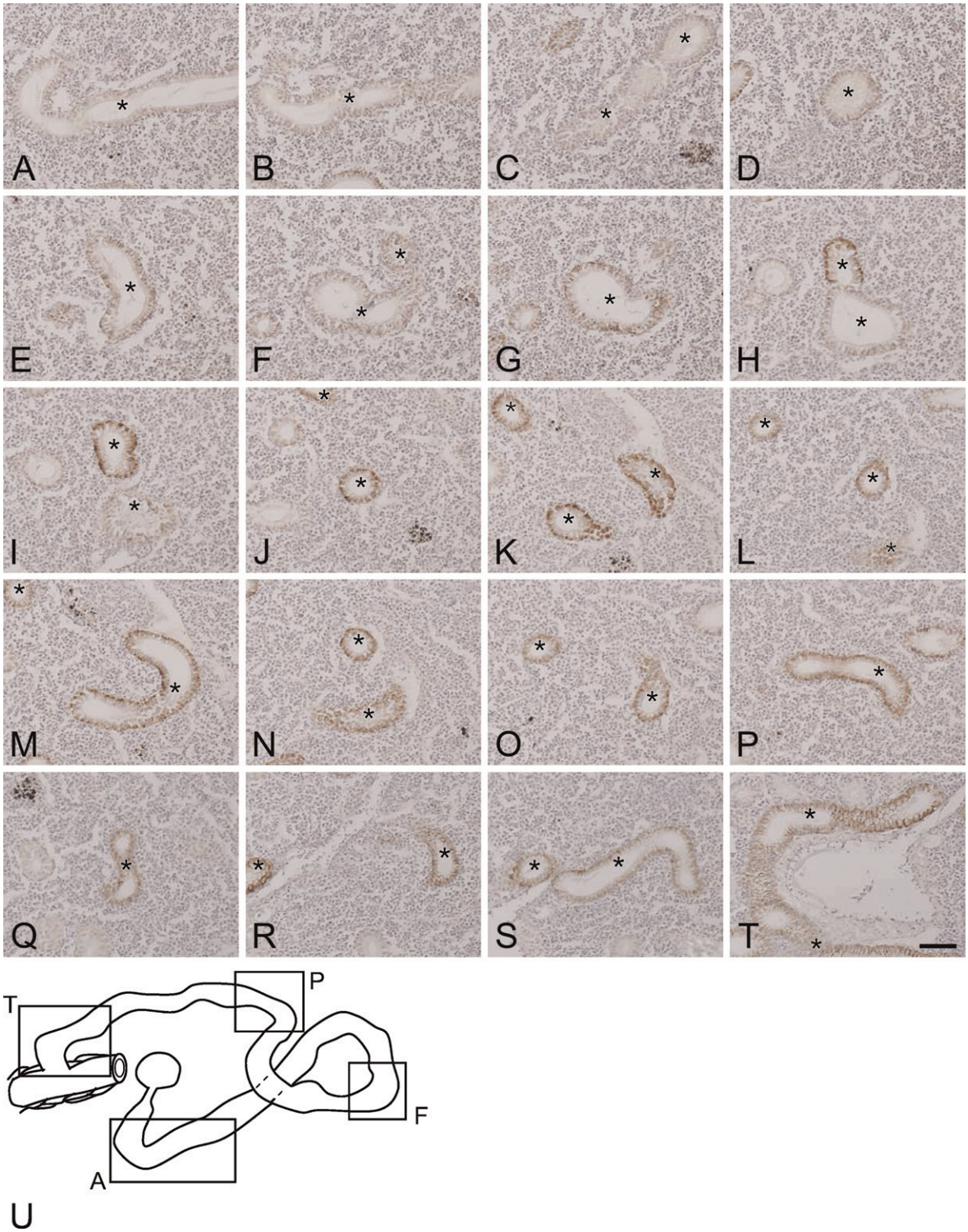

Figure 6 A series of representative sections (**A–T**) and the overlaid image (**U**) of a single nephron in the kidney of freshwater-acclimated eel. Serial paraffin sections were cut at 8-μm thickness and immunostained with anti-Na^+/K^+-ATPase. Asterisks indicate sections of a single nephron to be traced. Bar = 50 μm.

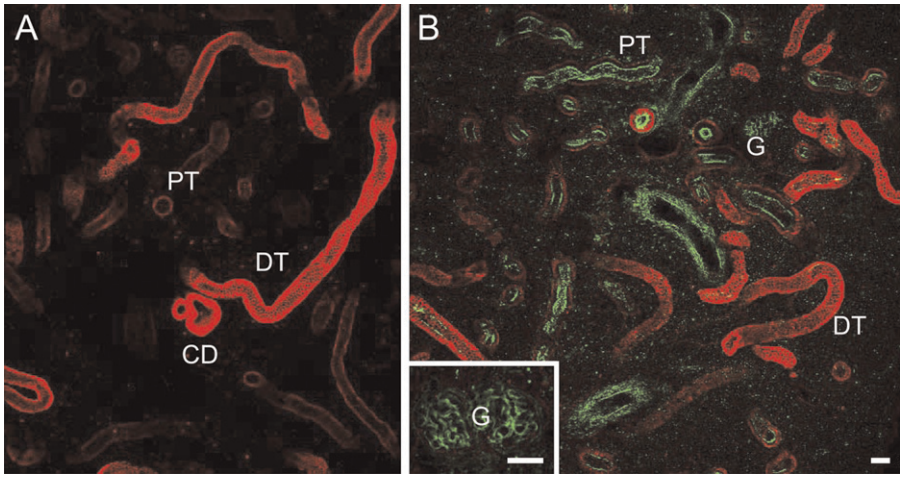

Figure 7 Confocal laser scanning micrographs of thick kidney slices (200-μm) of freshwater-acclimated eel, immunostained with anti-Na^+/K^+-ATPase (red, **A**) and double-stained with anti-Na^+/K^+-ATPase and wheat germ agglutinin (WGA) (green, **B**). Inset, magnified view of a WGA-positive glomerulus (G). PT, proximal tubule; DT, distal tubule; CD, collecting duct. Bar = 50 μm.

to seawater, indicating highly active ion uptake through mitochondria-rich cells in hypotonic environments (Katoh et al. 2001). In killifish, mitochondria-rich cells may complement the limited renal ability to retain monovalent ions for freshwater adaptation. In Japanese eels, the presence of distinct DT segments implies more-effective reabsorption of monovalent ions in the kidney, making hyperosmoregulation less dependent on mitochondria-rich cells.

Electron microscopic observations on the kidneys of freshwater and seawater eels further revealed the morphological characteristics of renal tubule cells, confirming the light microscopic observations. In addition, electron microscopic observations showed characteristic fine structures of renal tubule cells. Interestingly, the fine structures of renal tubule cells were similar between freshwater and seawater eels. First, the renal tubule cells were, in general, rich in mitochondria, and thus categorized as "mitochondria-rich cells," as is the case with gill mitochondria-rich cells (Evans et al. 2005). Among the different segments of the renal tubule, the DT cells were most abundant in mitochondria. In addition, the basal infolding was typically observed in the basal half of the cells in PT-I and PT-II segments, whereas the basolateral membrane in DT cells invaginated much more deeply than in PT-I and PT-II cells. Second, structural features of the PT segment, such as the presence of microvilli and lysosomal granules, are common between teleosts and mammals (Hickman and Trump 1969; Thoenes and Langer 1969; Fawcett 1994), suggesting a functional similarity of this segment between them. In the mammalian PT segment, it is thought that proteins reabsorbed by pinocytosis are degraded to amino acids in lysosomal granules, and that the resultant amino acids return to the blood circulation (Thoenes and Langer 1969). It is thus likely that the PT-I segment is also responsible for protein reabsorption in Japanese eel and other teleosts.

In the light-microscopic immunocytochemistry, we showed that the Na^+/K^+-ATPase immunoreaction was detected all along the renal tubule and CD, although the subcellular distribution varied among different segments of the renal tubules. In freshwater eel, whereas the faint Na^+/K^+-ATPase immunoreaction was restricted to the subcellular region along the basolateral membrane of PT cells, the immunoreaction was more intense in DT and CD cells. Ura et al. (1996) also reported immunocytochemical localization of Na^+/K^+-ATPase in the kidneys of masu salmon (*Oncorhynchus masou*), Japanese eel, and rockfish, (*Sebastes schlegeli*). In accordance with our observations, the Na^+/K^+-ATPase immunoreaction was observed along the renal tubule in those teleost species. In the present study, we further attempted electron microscopic immunocytochemistry for Na^+/K^+-ATPase in the eel kidney, which indicated that the Na^+/K^+-ATPase immunoreaction was distributed on the membranes of the basal infolding, continuous with the basolateral membrane of renal tubule cells. The specificity of the immunoreaction was confirmed by the control experiment, in which no immunoreaction was detected in the specimens incubated with the preimmune serum in place of the specific antiserum. The distribution pattern of Na^+/K^+-ATPase on the basolateral infolding was in accordance with that observed in the light microscopic immunocytochemistry.

Because Na^+/K^+-ATPase was shown to be expressed all along the renal tubule and CD, we adopted anti-Na^+/K^+-ATPase as a specific marker to follow the renal tubules running spatially in the kidney. Although some previous studies have described sectional images of renal tubules (Anderson and Loewen 1975; Katoh et al. 2008), limited information is available on the structure of sterically disposed renal tubules in the teleost kidney. For a better understanding of renal functions, we adopted freshwater-acclimated eel as a

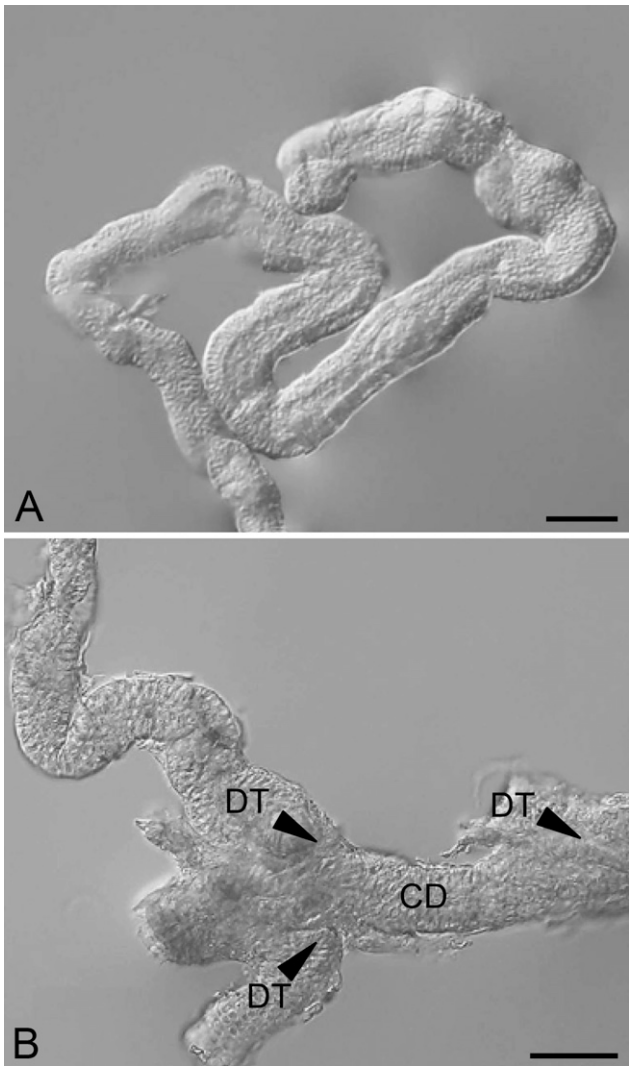

Figure 8 Nephrons dissociated from the kidney of freshwater-acclimated eel. **(A)** A renal tubule of a dissociated nephron, meandering in a random pattern. **(B)** After meandering, the distal tubules (DT) are merged into a collecting duct (CD), as indicated by arrowheads. Bar = 50 μm.

model for analysis of the three-dimensional structure of the nephron. The spatial alignment of the nephrons was examined by observations on serial paraffin sections and single thick slices (200 μm) immunostained with anti-Na^+/K^+-ATPase. On serial paraffin sections, we successfully followed all renal tubule segments, and different segments were readily distinguished by their morphological characteristics. On kidney slices, although it was difficult to distinguish between the PT-I and PT-II segments in the PTs with WGA-positive brush borders, the DT and CD segments without brush borders were distinct from the PT (PT-I and PT-II). The confocal laser scanning microscopic image of the kidney slice provided a clear picture, depicting the stereoscopic structure of renal tubules. Although the 200-μm slice was not thick enough to cover a whole nephron, those images allowed us to observe several nephrons at the same time. Both observations clearly indicated that the renal tubule meanders in a random pattern through lymphoid tissues. The spatial alignment of the renal tubules observed on serial paraffin sections and single thick slices was also supported by observations on dissociated single nephrons. Although the dissociated nephron was segmentalized and lost its in situ spatial distribution, a fragment of the renal tubule maintained its meandering alignment, often showing the sites where some renal tubules were merged into a CD.

Because the renal tubules in the eel kidney did not show any regular alignment, it is unlikely that renal tubules interact with each other. In contrast, it is well known that in other classes of vertebrates, the nephrons are arranged in a certain regular pattern, and that different segments interact with each other within a single nephron. In the nephrons of marine elasmobranch fishes, for example, the renal tubules with four loops form five closely adjacent tubular segments (Lacy and Reale 1995). Marine elasmobranches retain a large amount of urea in their blood plasma, whose osmolality is maintained at slightly higher than that of surrounding seawater to overcome osmotic water loss. In marine elasmobranches, reabsorption of urea from the primitive urine takes place in the complicated loop structure of the renal tubules, which acts as a countercurrent multiplier system to enhance urea reabsorption (Hyodo et al. 2004; Marshall and Grosell 2006). Similarly, the mammalian nephron has a regular loop structure of the renal tubules, the loop of Henle, which functions as a countercurrent multiplier and contributes to production of urine hyperosmotic to the plasma (Fawcett 1994; Iino et al. 2001). Those regularly arranged loop structures of marine elasmobranch and mammalian nephrons are distinct from randomly arranged teleost renal tubules. The lack of regularly arranged loop structures in the teleost kidney may be related to the inability to produce hyperosmotic urine, reflecting that their habitats and adaptive strategies are different from those of elasmobranch and mammalian species.

The extensive expression of Na^+/K^+-ATPase along the renal tubules suggests its involvement in active transport of ions and other solutes between the primitive urine and body fluid. Among the different segments, the DT and CD cells showed more-intense Na^+/K^+-ATPase immunoreaction in freshwater eel than in seawater eel, suggesting that the DT and CD segments are important in freshwater adaptation, or hyperosmoregulation. In our observations, whereas the general structure of renal tubules examined at both light and electron microscopic levels is similar

between freshwater and seawater eels, the Na^+/K^+-ATPase immunoreaction varied greatly between them. These findings suggest that the regulation of gene and protein expression of Na^+/K^+-ATPase is the primary cause of the salinity-dependent change in the DT segment. It is generally accepted that the DT is responsible for reabsorption of monovalent ions such as Na^+ and Cl^- from primitive urine in the kidney of freshwater fish (Nishimura et al. 1983; Nishimura and Fan 2003). In Mozambique tilapia, Miyazaki et al. (2002) identified a kidney-specific chloride channel (CLC-K), whose mRNA expression levels were higher in freshwater fish than in seawater fish. The immunocytochemical study also showed that the CLC-K immunoreaction was localized on the structure of the basolateral membrane infolding in the DT cells, suggesting CLC-K is involved in Cl^- reabsorption in the DT of freshwater-adapted tilapia. On the basis of our finding that Na^+/K^+-ATPase is also localized on the basal infolding more intensely in freshwater eel than in seawater eel, it is most likely that Na^+ and Cl^- reabsorption is driven by basolateral Na^+/K^+-ATPase in the DT segment. In addition to the DT segment, the CD expressing Na^+/K^+-ATPase is considered to be an additional site of monovalent ion reabsorption (Marshall and Grosell 2006). On the other hand, previous studies have shown that seawater acclimation increased gene expression and activity of Na^+/K^+-ATPase (Cutler et al. 1995,2000; Marsigliante et al. 2000), which may be related to secretion of divalent ions in the PT segments for adaptation to hypertonic environments.

In marine teleost fishes, the PT-I segment is thought to secrete divalent ions for adaptation to hypertonic environments (Beyenbach 1995). For example, Katoh et al. (2006) have proposed a sulfate-secreting mechanism driven by Na^+/K^+-ATPase and vacuolar-type H^+-ATPase in the PT-I segment of the rainbow trout kidney. Meanwhile, PT-II segments are involved in reabsorption of glucose and other organic solutes (Marshall and Grosell 2006), which is independent of osmoregulation and ion regulation. Thus, the secretion and reabsorption of ions and other solutes along the renal tubules have an important involvment not only in osmoregulation but also in other physiological events. It could be concluded that Na^+/K^+-ATPase expressed all along the renal tubules and CD provides, at least in part, the driving forces for active solute transports for osmoregulation and other biological events in the kidney.

Literature Cited

Anderson BG, Loewen RD (1975) Renal morphology of freshwater trout. Am J Anat 143:93–114

Beyenbach KW (1995) Secretory electrolyte transport in renal proximal tubules of fish. In Wood CM, Shuttleworth TJ, eds. Cellular and Molecular Approaches to Fish Ionic Regulation. San Diego, Academic Press, 85–105

Cutler CP, Brezillon S, Bekir S, Sanders IL, Hazon N, Cramb G (2000) Expression of a duplicate Na,K-ATPase beta(1)-isoform in the European eel (Anguilla anguilla). Am J Physiol 279: R222–229

Cutler CP, Cramb G (2008) Differential expression of absorptive cation-chloride-cotransporters in the intestinal and renal tissues of the European eel (Anguilla anguilla). Comp Biochem Physiol B Biochem Mol Biol 149:63–73

Cutler CP, Sanders IL, Hazon N, Cramb G (1995) Primary sequence, tissue specificity and expression of the Na+,K(+)-ATPase alpha 1 subunit in the European eel (Anguilla anguilla). Comp Biochem Physiol B Biochem Mol Biol 111:567–573

Edwards JG, Schnitter C (1933) The renal unit in the kidney of vertebrates. Am J Anat 53:55–88

Evan AP, Dail WG, Dammrose D, Palmer C (1976) Scanning electron microscopy of cell surfaces following removal of extracellular material. Anat Rec 185:433–445

Evans DH, Piermarini PM, Choe KP (2005) The multifunctional fish gill: dominant site of gas exchange, osmoregulation, acid-base regulation, and excretion of nitrogen waste. Physiol Rev 85:97–177

Fawcett DW (1994) The urinary system. In Bloom W, Fawcett DW, eds. A Textbook of Histology. 12th ed. New York, Chapman and Hall, 728–767

Geering K (1990) Subunit assembly and functional maturation of Na,K-ATPase. J Membr Biol 115:109–121

Hickman CP Jr (1968) Ingestion, intestinal absorption, and elimination of seawater and salts in the southern flounder, Paralichthys lethostigma. Can J Zool 46:457–466

Hickman CP Jr, Trump BF (1969) The kidney. In Hoar WS, Randall DJ, eds. Fish Physiology, vol. 1. New York, Academic Press, 91–239

Hiroi J, McCormick SD (2007) Variation in salinity tolerance, gill Na^+/K^+-ATPase, $Na^+/K^+/2Cl^-$ cotransporter and mitochondria-rich cell distribution in three salmonids Salvelinus namaycush, Salvelinus fontinalis and Salmo salar. J Exp Biol 210:1015–1024

Hiroi J, Yasumasu S, McCormick SD, Hwang PP, Kaneko T (2008) Evidence for an apical Na-Cl cotransporter involved in ion uptake in a teleost fish. J Exp Biol 211:2584–2599

Hirose S, Kaneko T, Naito N, Takei Y (2003) Molecular biology of major components of chloride cells. Comp Biochem Physiol B Biochem Mol Biol 136:593–620

Hsu SM, Raine L, Fanger H (1981) Use of avidin-biotin-peroxidase complex (ABC) in immunoperoxidase techniques: a comparison between ABC and unlabeled antibody (PAP) procedures. J Histochem Cytochem 29:577–580

Hwang PP, Fang MJ, Tsai JC, Huang CJ, Chen ST (1998) Expression of mRNA and protein of Na^+, K^+-ATPase α subunit in gills of tilapia (Oreochromis mossambicus). Fish Physiol Biochem 18:363–373

Hwang PP, Lee TH (2007) New insights into fish ion regulation and mitochondrion-rich cells. Comp Biochem Physiol A Mol Integr Physiol 148:479–497

Hyodo S, Katoh F, Kaneko T, Takei Y (2004) A facilitative urea transporter is localized in the renal collecting tubule of the dogfish Triakis scyllia. J Exp Biol 207:347–356

Iino N, Gejyo F, Arakawa M, Ushiki T (2001) Three-dimensional analysis of nephrogenesis in the neonatal rat kidney: light and scanning electron microscopic studies. Arch Histol Cytol 64:179–190

Inokuchi M, Hiroi J, Watanabe S, Lee KM, Kaneko T (2008) Gene expression and morphological localization of NHE3, NCC and NKCC1a in branchial mitochondria-rich cells of Mozambique tilapia (Oreochromis mossambicus) acclimated to a wide range of salinities. Comp Biochem Physiol A Mol Integr Physiol 151: 151–158

Katoh F, Cozzi RR, Marshall WS, Goss GG (2008) Distinct $Na^+/K^+/2Cl^-$ cotransporter localization in kidneys and gills of two euryhaline species, rainbow trout and killifish. Cell Tissue Res 334:265–281

Katoh F, Hasegawa S, Kita J, Takagi Y, Kaneko T (2001) Distinct seawater and freshwater types of chloride cells in killifish, Fundulus heteroclitus. Can J Zool 79:822–829

Katoh F, Shimizu A, Uchida K, Kaneko T (2000) Shift of chloride cell distribution during early life stages in seawater-adapted killifish, Fundulus heteroclitus. Zoolog Sci 17:11–18

Katoh F, Tresguerres M, Lee KM, Kaneko T, Aida K, Goss GG (2006) Cloning of rainbow trout SLC26A1: involvement in renal sulfate secretion. Am J Physiol 290:R1468–1478

Lacy ER, Reale E (1995) Functional morphology of the elsasmobranch nephron and retention of urea. In Wood CM, Shuttleworth TJ, eds. Cellular and Molecular Approaches to Fish Ionic Regulation. San Diego, Academic Press, 107–146

Lee KM, Kaneko T, Aida K (2005) Low-salinity tolerance of juvenile fugu Takifugu rubripes. Fish Sci 71:1322–1329

Lucu C, Flik G (1999) Na^+K^+-ATPase and Na^+/Ca^{2+} exchange activities in gills of hyperregulating Carcinus maenas. Am J Physiol 45:R490–499

Marshall WS, Grosell M (2006) Ion transport, osmoregulation, and acid-base balance. In Evans D, Claiborne JB, eds. The Physiology of Fishes. 3rd ed. New York, CRC Press, 179–230

Marsigliante S, Muscella A, Barker S, Storelli C (2000) Angiotensin II modulates the activity of the Na+/K+ATPase in eel kidney. J Endocrinol 165:147–156

Miyazaki H, Kaneko T, Uchida S, Sasaki S, Takei Y (2002) Kidney-specific chloride channel, OmClC-K, predominantly expressed in the diluting segment of freshwater-adapted tilapia kidney. Proc Natl Acad Sci USA 99:15782–15787

Nishimura H, Fan Z (2003) Regulation of water movement across vertebrate renal tubules. Comp Biochem Physiol A Mol Integr Physiol 136:479–498

Nishimura H, Imai M, Ogawa M (1983) Sodium chloride and water transport in the renal distal tubule of the rainbow trout. Am J Physiol 244:F247–254

Ojeda JL, Icardo JM, Domezain A (2003) Renal corpuscle of the sturgeon kidney: an ultrastructural, chemical dissection, and lectin-binding study. Anat Rec A Discov Mol Cell Evol Biol 272:563–573

Sasai S, Katoh F, Kaneko T, Tsukamoto K (2007) Ontogenic change of gill chloride cells in leptocephalus and glass eel stages of the Japanese eel, Anguilla japonica. Mar Biol 150:487–496

Thoenes W, Langer KH (1969) Relationship between cell structures of renal tubules and transport mechanisms. In Thurau K, Jahrmarkes H, eds. Renal Transport and Diuretics. Berlin, Springer, 37–65

Uchida K, Kaneko T, Miyazaki H, Hasegawa S, Hirano T (2000) Excellent salinity tolerance of Mozambique tilapia (Oreochromis mossambicus): elevated chloride cell activity in the branchial and opercular epithelia of the fish adapted to concentrated seawater. Zoolog Sci 17:149–160

Uchida K, Kaneko T, Yamauchi K, Hirano T (1996) Morphometrical analysis of chloride cell activity in the gill filaments and lamellae and changes in Na^+, K^+-ATPase activity during seawater adaptation in chum salmon fry. J Exp Zool 276:193–200

Ura K, Soyano K, Omoto N, Adachi S, Yamauchi K (1996) Localization of Na^+, K^+-ATPase in tissues of rabbit and teleosts using an antiserum directed against a partial sequence of the α-subunit. Zoolog Sci 13:219–227

Watanabe S, Niida M, Maruyama T, Kaneko T (2008) Na^+/H^+ exchanger isoform 3 expressed in apical membrane of gill mitochondrion-rich cells in Mozambique tilapia Oreochromis mossambicus. Fish Sci 74:813–821

Wright CS (1984) Structural comparison of the two distinct sugar binding sites in wheat germ agglutinin isolectin II. J Mol Biol 178:91–104

The Journal of Histochemistry & Cytochemistry